0026-895X/05/6806-1728–1735$20.00
MOLECULAR PHARMACOLOGY
Copyright © 2005 The American Society for Pharmacology and Experimental Therapeutics
*Mol Pharmacol* 68:1728–1735, 2005

Vol. 68, No. 6
13870/3064370
*Printed in U.S.A.*



# Identification and Selective Inhibition of the Channel Mode of the Neuronal GABA Transporter 1

Stephan Krause[1] and Wolfgang Schwarz

*Max-Planck-Institute for Biophysics, Frankfurt am Main, Germany; and Max-Planck Guest Laboratory at the Institute of Biochemistry and Cell Biology, Chinese Academy of Sciences, Shanghai, China*

Received April 19, 2005; accepted September 7, 2005

## ABSTRACT

The function of GAT1, the transporter for the inhibitory neurotransmitter GABA, is characterized by expression in *Xenopus laevis* oocytes and measurements of GABA-induced uptake of [$^3$H]GABA, $^{22}Na^+$, and $^{36}Cl^-$, and GABA-evoked currents under voltage-clamp conditions. *N*-[4,4-Diphenyl-3-butenyl]-nipecotic acid (SKF-89976-A), a specific inhibitor of GAT1, is used in our system as a pharmacological tool. The GABA-evoked current can be decomposed into a transport current, which is coupled to the GABA uptake, and a transmitter-gated current, which is uncoupled from the GABA uptake. The transport current results from a fixed stoichiometry of 1 GABA/2 $Na^+$/1 $Cl^-$ transported during each cycle, as determined by radioactive tracer flux measurements. The transmitter-gated current is mediated by an $Na^+$-conductance pathway. As a competitive inhibitor for GABA uptake, SKF-89976-A can separate the two current components. The GABA uptake is blocked with a $K_I$ value of approximately 7 $\mu$M, whereas the uncoupled transmitter-gated current is inhibited with a $K_I$ value of approximately 0.03 $\mu$M. Thus, the results of this study not only identify the transport mode and the channel mode of GAT1 but also raise the possibility of separating these components in a physiological environment.

In the mammalian central nervous system, neurotransmitter-evoked synaptic signals are mainly terminated by the diffusion of the neurotransmitter out of the synaptic cleft and by active uptake into the presynaptic nerve terminals and surrounding glia cells by means of neurotransmitter transporters. Dramatic effects of specific inhibitors of the transporters suggest that they play the dominant role in the termination of the synaptic activity (Masson et al., 1999). Thus, detailed knowledge of their function is essential for understanding the physiology of synaptic transmission.

We investigated the GABA transporter 1 of mouse brain (mGAT1) belonging to the family of secondary active transport systems that are driven by electrochemical gradients for $Na^+$ and $Cl^-$ (Kanner, 1978; Kavanaugh et al., 1992; Nelson, 1998). Most members of this family share the property that the current generated by the activity of transporters consists of three components that were named transport current (Sonders and Amara, 1996), transmitter-gated current (Galli et al., 1997), and transmitter-independent leak current (Sonders and Amara, 1996). The transport current is caused by translocation of net charges attributable to cotransport of $Na^+$ and $Cl^-$ ions along with the substrate, which is generally assumed to occur at a fixed stoichiometry. The transmitter-gated current is not associated with translocation of the respective neurotransmitter, although the binding of the substrate to the transporter is essential. The third component, the transmitter-independent leak current, can be detected in the absence of transmitter and is supposed to be carried by alkali ions (Sonders and Amara, 1996); in the case of the GAT1 expressed in human embryonic kidney cells, single-channel events could be observed in the absence of GABA (Cammack and Schwartz, 1996). Current components that are not related to neurotransmitter uptake have also been found in other transporter families (Sonders and Amara, 1996).

For the family of $Na^+/Cl^-$-dependent neurotransmitter transporters, the different modes of transporter-mediated current have been described in detail for the norepinephrine transporter (Galli et al., 1995, 1996), the serotonin transporter (Mager et al., 1994; Galli et al., 1997), and the dopamine transporter (Sonders et al., 1997; Ingram et al., 2002). As an exception, the glycine transporter seems not to exhibit transmitter-gated current (Supplisson and Roux, 2002; Aragon and Lopez-Corcuera, 2003). Whereas in their series of

Part of this work was supported on the basis of an agreement between the Chinese Academy of Sciences and the Max-Planck Gesellschaft.

[1]Current affiliation: University of Oulu, Department of Physical Sciences, Division of Biophysics, Oulun Yliopisto, Finland.

Article, publication date, and citation information can be found at http://molpharm.aspetjournals.org.
doi:10.1124/mol.105.013870.

**ABBREVIATIONS:** GAT1, GABA transporter isoform 1; m, mouse; NA, nipecotic acid; PMZ, promethazine; SKF, SKF-89976-A (*N*-[4,4-diphenyl-3-butenyl]-nipecotic acid); MOPS, 4-morpholinepropanesulfonic acid.

studies on GAT1 in *Xenopus laevis* oocytes, Lu and Hilgemann (Hilgemann and Lu, 1999; Lu and Hilgemann, 1999a,b) did not find evidence for additional current components, others observed in HeLa cells GAT1-mediated currents that are not linked to the transport of GABA (Risso et al., 1996). In addition, the finding of Eckstein-Ludwig et al. (1999) that tiagabine differently inhibits GABA uptake and GABA-evoked current has been judged as an indication for an additional current component.

In the work presented here, we show first that the steady-state current of mGAT1 evoked by GABA (GABA-evoked current) consists of two components, the transport current and the transmitter-gated current, with the latter mediated by a $Na^+$ conductance. Second, we characterize the inhibition of mGAT1 by the specific inhibitor SKF-89976-A (SKF) (Borden et al., 1995) and show that this drug can be a powerful tool to separate transport current and transmitter-gated current. Finally, we show by direct flux measurements that the transport stoichiometry of the mGAT1 is indeed 1 GABA/2 $Na^+$/1 $Cl^-$, which until now has been estimated roughly either indirectly from the analysis of the respective Hill coefficients (Kavanaugh et al., 1992) or from uptake measurements under various conditions (Keynan and Kanner, 1988; Loo et al., 2000).

## Materials and Methods

**Expression of mGAT1 in *X. laevis* Oocytes.** Full-grown prophase-arrested oocytes were isolated from female *X. laevis* and treated with 3 or 1.5 U/10 ml Liberase (Roche Diagnostics, Mannheim, Germany) for 2 to 4 h or overnight, respectively. mGAT1 was expressed in the oocytes by injection of 23 ng of cRNA per cell. Experiments were done after 3 days of incubation at 19°C. All experiments were conducted in climate-controlled rooms at a room temperature of 25°C.

**Voltage-Clamp Experiments.** Electrophysiological experiments were performed on the oocytes with the conventional two-electrode voltage clamp (Lafaire and Schwarz, 1986) using Turbo TEC-03 or -10 amplifiers and CellWorks software (NPI Electronic GmbH, Tamm, Germany). For measuring GABA-evoked steady-state currents of mGAT1, membrane currents were recorded during the last 80 ms of 400-ms rectangular voltage pulses from −150 to +30 mV in 10-mV increments applied from a holding potential of −60 mV. The difference between steady-state currents in the presence of extracellular GABA and in its absence was taken as a measure of the GABA-evoked current. For measuring mGAT1-mediated charge movements, transient currents were integrated, which were elicited with rectangular voltage steps from 400-ms prepulses in the range of −150 to +30 mV in 10-mV increments and back to the holding potential of −60 mV. The difference between the integrals in the absence of extracellular GABA and in its presence was taken as a measure of the mGAT1-mediated charge movement in the absence of GABA. In all experiments, the current was filtered at 100 Hz and sampled at 1 kHz.

**Radioactive Tracer Measurements.** For measurements of radioactive tracer uptake, 10 to 20 oocytes were incubated in 200 $\mu$l of the respective tracer solution for 10 min. Within this time span, uptake showed linear time dependence. For GABA uptake [$^3$H]GABA (9.25 kBq/200 $\mu$l) was used; for $Na^+$ uptake, $^{22}Na^+$ (74 kBq/200 $\mu$l); for $Cl^-$ uptake, $^{36}Cl^-$ (90.6 kBq/200 $\mu$l); and for $Rb^+$ uptake, $^{86}Rb^+$ (0.57 kBq/50 $\mu$l; all from GE Healthcare, Little Chalfont, Buckinghamshire, UK). After the incubation, the oocytes were washed, placed individually into counting vials, and dissolved in 0.1 ml (5%) SDS solution. The radioactivity taken up by the oocytes was then determined by liquid scintillation counting. Rates of uptake of control oocytes, which were not injected with mGAT1 cRNA, were subtracted from rates of uptake of mGAT1-expressing oocytes.

For [$^3$H]GABA uptake measurements under voltage clamp, single oocytes were clamped for 10 min to the respective holding potential, and the corresponding holding currents were recorded on a pen recorder. The bath volume of the measuring chamber was approximately 700 $\mu$l and contained 37 kBq [$^3$H]GABA. The radioactivity taken up by an oocyte was determined as described above. Rates of uptake of control oocytes, which were not injected with mGAT1 cRNA, were subtracted from rates of uptake of mGAT1-expressing oocytes. The current calculated from [$^3$H]GABA uptake under voltage-clamp control was performed as follows: for each clamped oocytes, 1 $\mu$l of bath solution was taken as a control sample and was treated exactly as described above for oocytes. Because the [$^3$H]GABA uptake measurements were performed at a GABA concentrations of 400 $\mu$M, the activity of 1 $\mu$l of bath solution determined by liquid scintillation counting was proportional to 400 pmol GABA. The amount of GABA taken up into each single oocyte ($m$) could then be calculated by rule of proportion according to the following equation:

$$m = \frac{400 \times 10^{-12} \times \text{activity (oocyte)}}{\text{activity (bath solution)}}$$

Assuming one transported net charge per GABA molecule per transport cycle (Keynan and Kanner, 1988; Kavanaugh et al., 1992), the transport current could then be calculated by

$$\frac{m \times F}{600} = I$$

where $m$ is the amount of GABA taken up into the oocyte (in moles), $F$ is the Faraday constant (in coulombs per mole), $400 \times 10^{-12}$ is the amount of GABA per 1 $\mu$l of bath solution (in moles), 600 is the uptake time (in seconds), and $I$ is the transport current (in amperes).

**Solutions.** The oocyte Ringer's solution was composed of 90 mM NaCl, 2 mM KCl, 2 mM $CaCl_2$, and 5 mM MOPS, and pH was adjusted with NaOH to pH 7.4. All compounds were from Sigma-Aldrich (Taufkirchen, Germany). SKF-89976-A was a generous gift of Glaxo SmithKline (Welwyn Garden City, Hertfordshire, UK). A GABA concentration of 400 $\mu$M was chosen to saturate the GABA-evoked current, also at hyperpolarized negative potentials (Grossman and Nelson, 2002).

**Data Analysis.** If not stated otherwise, normalization and averaging of the data were performed as follows: before averaging GABA-evoked currents, all GABA-evoked currents of each single oocyte were normalized to the GABA-evoked current in the presence of 400 $\mu$M GABA at −100 mV of the respective oocyte. Before averaging rates of uptake, the rate for each single oocyte was normalized to the averaged rate of uptake of the respective batch of oocytes in the presence of 400 $\mu$M GABA. All curve fittings were performed by least square fits. Analysis of data was performed using Origin 7.0 (OriginLab Corp., Northampton, MA).

**Definitions.** *GABA-evoked current* is the current observed by the addition of GABA to the transporter. It can be decomposed into two components: transport current, and transmitter-gated current. *Transport current* is a component of the GABA-evoked current, which is coupled to GABA uptake. *Transmitter-gated current* is a second component of the GABA-evoked current, which is unrelated to GABA uptake and is believed to be caused by $Na^+$ conduction through the transporter. *Current calculated from GABA uptake* is an expected value of the transport current. GABA uptake is measured and the data are converted to current based on a fixed stoichiometry of 1 GABA:2 $Na^+$:1 $Cl^-$. *Steady-state current* is a term representing the current near the end of voltage pulses. The difference of steady-state currents in the presence of GABA and its absence represents the GABA-evoked current. *Transient current* represents the capacitance current measured after the onset of a voltage pulse. The integral obtained in the absence of GABA represents the charges

transferred within the electric field associated with transition of the transporter between $Na^+$-unbound and -bound states.

## Results

In *X. laevis* oocytes expressing mGAT1, the application of GABA induced an inward-directed, voltage-dependent current (GABA-evoked current) (Fig. 1A). In the presence of 400 $\mu$M GABA, the GABA-evoked current (Fig. 1B, ■) was greater than the current calculated from the voltage-clamp controlled GABA uptake (●) by a factor of 3 to 5 over the entire potential range, assuming a coupling stoichiometry of 1 GABA:2 $Na^+$:1 $Cl^-$ (Keynan and Kanner, 1988; Kavanaugh et al., 1992). The current-voltage curve in the presence of 400 $\mu$M GABA and 25 $\mu$M SKF (broken line) shows little deviation from the calculated current over the entire voltage range from −20 to −80 mV. To clarify the inhibiting properties of SKF, [$^3$H]GABA uptake and GABA-evoked current on SKF concentration were recorded. Figure 2 shows that GABA uptake and GABA-evoked current are differently inhibited. The uptake measurements in Fig. 2 were not performed under voltage-clamp control. To compare these uptake measurements with GABA-evoked current, we used the GABA-evoked current at −20 mV, which is close to the resting potential of mGAT1-expressing oocytes in the presence of 400 $\mu$M GABA (data not shown). Whereas 50% inhibition of the GABA-evoked current was obtained at $IC_{50}$ (current) = 1.5 $\mu$M SKF, 36 times higher concentrations were needed for 50% inhibition of the rate of uptake [$IC_{50}$ (uptake) = 54 $\mu$M SKF]. A transmitter-independent leak current in the absence of GABA, which has been reported in human embryonic kidney cells expressing GAT1 (Cammack and Schwartz, 1996) was not detected in oocytes (U. Eckstein-Ludwig and J. Rettinger, personal communication).

The molecule SKF consists of two major moieties, a GABA-analogous part, which naturally can be believed to bind to the GABA binding site of the transporter, and a planar ring system, which usually is assumed to interact with aromatic amino acids. Figure 3 compares the $IC_{50}$ values for inhibition of rate of uptake and of GABA-evoked current by SKF with those of other mGAT1-inhibiting compounds that have typical structural moieties in common with SKF. $IC_{50}$ values for GABA-evoked current and rate of uptake were obtained under the conditions as particularly described for SKF (see above). Whereas nipecotic acid (NA), which represents the GABA-analogous residue of SKF, inhibited the GABA-evoked current with an $IC_{50}$ (current) of 20 $\mu$M, 1 order of magnitude higher concentration was needed for 50% inhibition of the rate of uptake [$IC_{50}$ (uptake) = 384 $\mu$M]. Promethazine (PMZ), with structural moiety analogous to the planar ring system of SKF, showed no remarkable difference in the $IC_{50}$ values for the inhibition of uptake (790 $\mu$M) and current (750 $\mu$M). The results of the experiments with PMZ, NA, and SKF suggest that 1) GABA-evoked current and GABA uptake do not represent the same process (see $IC_{50}$ values); 2) the difference in GABA-evoked current and GABA uptake can be attributed to a transport current and a transmitter-gated current (for detailed explanation, see *Discussion*); and 3) GABA uptake and GABA-evoked current are inhibited by interference of a GABA-analogous moiety interacting with the GAT1 protein.

Because the effect of SKF on GABA uptake can be described by a competitive inhibition (Fig. 4A), the following equation was used to fit rates of uptake in Fig. 2:

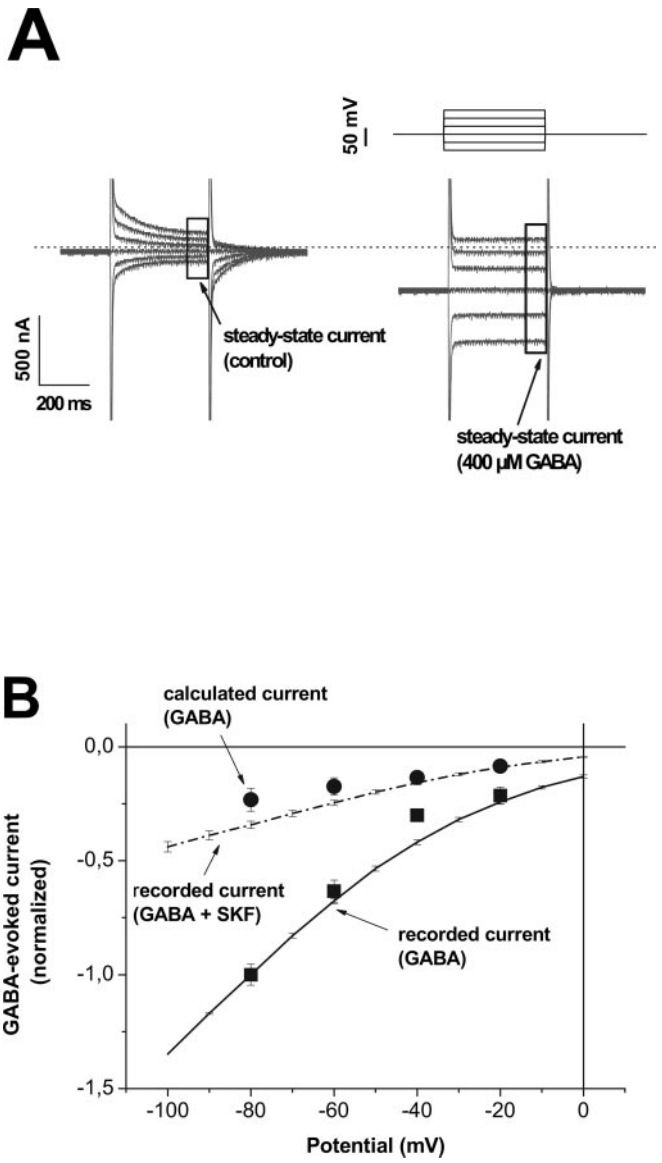


**Fig. 1.** Voltage-dependence of GABA-evoked current. A, typical current responses of a single mGAT1-expressing oocyte to 400-ms voltage pulses from −100 to 0 mV in 20-mV increments applied from a holding potential of −60 mV. The left traces are recorded in the absence of GABA, the right traces in the presence of 400 $\mu$M GABA. The broken line represents the 0 nA current level. Differences of steady-state currents in the presence of GABA and its absence are plotted in B as GABA-evoked current. Because of the scaling, the capacitive peaks of the oocytes are cut. B, ●, current calculated from rate of GABA uptake measured under voltage clamp. The current of each single oocyte was calculated separately. ■, respective recorded GABA-evoked current at 400 $\mu$M GABA. Data are averages ± S.E.M. from five oocytes. The solid line connects data of GABA-evoked currents at 400 $\mu$M GABA from other sets of oocytes in the absence of SKF. Data are averages of 28 oocytes ± S.E.M. The broken line connects data of GABA-evoked currents at 400 $\mu$M GABA in the presence of 25 $\mu$M SKF. Data are averages of 10 oocytes ± S.E.M. All curves are normalized to the value at 400 $\mu$M GABA and −80 mV in the absence of SKF. In the case of oocyte sets used in uptake measurements (■ and ●), current and uptake were recorded for 10 min, and one unit corresponds to −90 ± 4 nA; during the recording time, the GABA-evoked current did not show any considerable decay. In the case of oocyte sets used in electrophysiological recordings in the absence and presence of SKF (solid line and broken line, respectively) currents were recorded for 400 ms (as described in A), and one unit corresponds to −200 ± 41 nA.

$$v = V_{max}^{transp} \frac{\frac{[GABA]}{K_m^{transp}}}{1 + \frac{[GABA]}{K_m^{transp}} + \frac{[SKF]}{K_I^{transp}}}$$

with $K_m^{transp}$ representing the $K_m$ value for uptake stimulation by GABA and $K_I^{transp}$ the $K_I$ value for inhibition of uptake by SKF. Fitting eq. 1 to the uptake data in Fig. 2 (○), a $K_I^{transp}$ = 7.6 μM was obtained [the $K_m^{transp}$ value was determined from the data in Fig. 4A (●) in the absence of SKF to 62 μM].

The inhibition of GABA-evoked current by SKF could only be described by the sum of two independent inhibitory reactions:

$$v = V_{max}^{transp} \frac{\frac{[GABA]}{K_m^{transp}}}{1 + \frac{[GABA]}{K_m^{transp}} + \frac{[SKF]}{K_I^{transp}}} + V_{max}^{trans\text{-}gate} \frac{\frac{[GABA]}{K_m^{trans\text{-}gate}}}{1 + \frac{[GABA]}{K_m^{trans\text{-}gate}} + \frac{[SKF]}{K_I^{trans\text{-}gate}}}$$

The superscript *transp* refers to the same parameter as in eq. 1, and *trans-gate* refers to the respective parameters for the

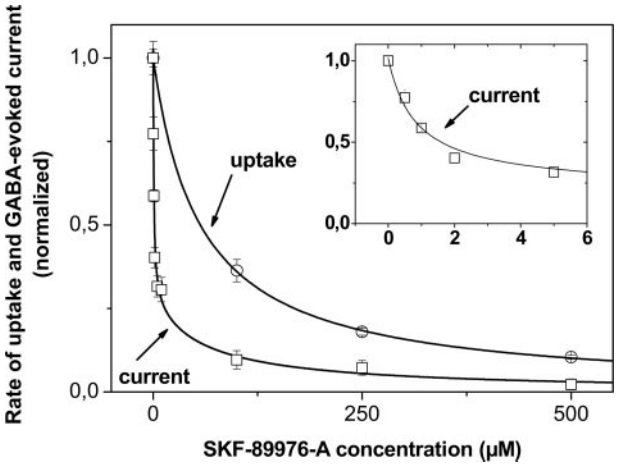


**Fig. 2.** Dependence of GABA-evoked current and rate of uptake in the presence of 400 μM GABA on SKF concentration. □, steady-state currents at −20 mV. Data are averages of three to eight oocytes ± S.E.M. The inset scales up the SKF-dependence of the GABA-evoked current in the range from 0 to 5 μM SKF. ○, rate of uptake of GABA. Data are averages of 30 oocytes ± S.E.M. Data sets for current and uptake are normalized to the value at 0 μM SKF. In the case of the steady-state currents at −20 mV, one unit corresponds to 43 ± 8.6 nA; in the case of rate of uptake, one unit corresponds to 275 ± 22 fmol/s. The lines are fits of eqs. 2 and 1, respectively, to the data points. The fitted parameters are listed in Table 1.

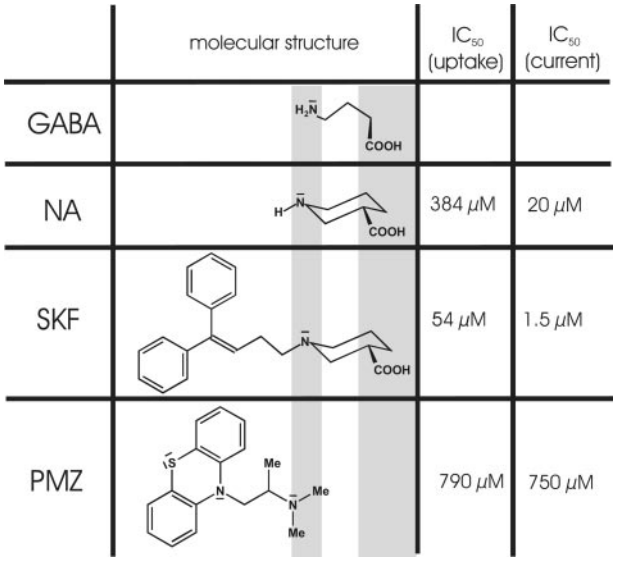


**Fig. 3.** $IC_{50}$ values of GAT1 inhibitors. SKF and NA share the same GABA-like structural moiety. The moieties of the inhibitors, particularly the Lewis base and the Lewis acid, are underlain in gray. The additional planar ring system of SKF is found in promethazine.

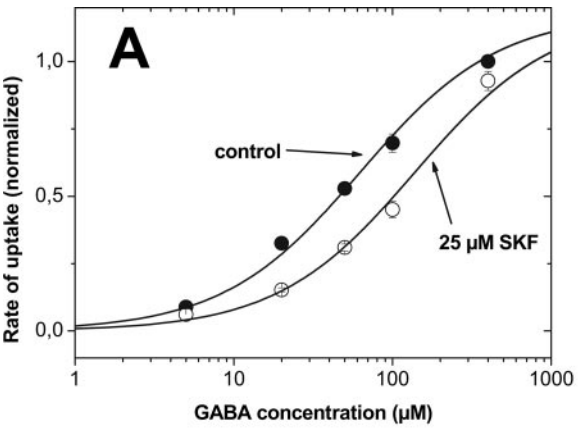


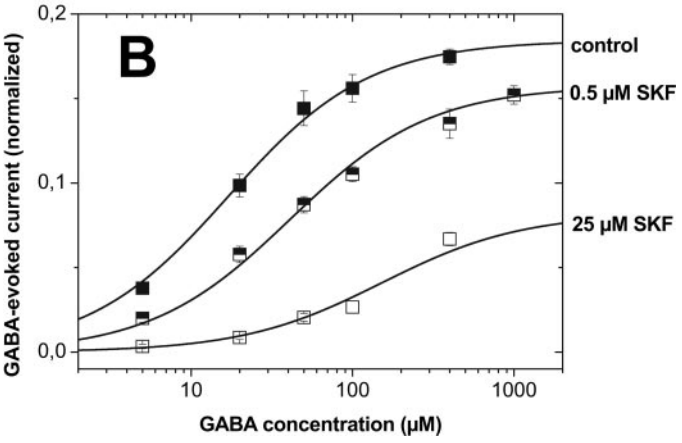


**Fig. 4.** Dependence on GABA concentration of GABA-evoked current and rate of uptake in the presence and absence of SKF. A, ●, rates of uptake of GABA in the absence of SKF. ○, rates of uptake of GABA in the presence of 25 μM SKF. Data represent the averages of 16 to 58 oocytes ± S.E.M. One unit corresponds to a rate of uptake of 433 ± 26 fmol/s. The lines represent the fits according to eq. 3. B, ■ represent GABA-evoked currents at −20 mV in the absence of SKF, half-open squares in the presence of 0.5 μM SKF, and □ in the presence of 25 μM SKF. Data are averages of 5 to 10 oocytes ± S.E.M. Data sets are normalized to the value at 400 μM GABA and −100 mV in the absence of SKF. One unit corresponds to a current of 264 ± 69 nA. The lines are fits according to eq. 3. The fitted parameters are listed in Table 1.

transmitter-gated current. The data for GABA-evoked current could be fitted with $K_I^{transp} = 8.8\ \mu M$ and $K_I^{trans\text{-}gate} = 0.03\ \mu M$ (using for the $K_m^{transp}$ and $K_m^{trans\text{-}gate}$ the values of Fig. 4, A and B, in the absence of SKF). The fitted value for $K_I^{transp}$ of GABA-evoked current was nearly identical with the value obtained directly from the uptake measurements.

For further characterization of the inhibitory effect of SKF on the uptake and the GABA-evoked current, we performed the corresponding experiments for the dependence on GABA concentration (Fig. 4, A and B) in the absence (filled symbols) and presence (open symbols) of SKF. Although the GABA-evoked current consists of two components, the results of the GABA concentration dependence did not allow realistic fits by the two-component equation (eq. 2), neither in the absence of SKF nor in the presence of SKF. This certainly is caused by the fact that the $K_m$ values for activation of the two components by GABA differ by less than a factor of 10, whereas the $K_I$ values for inhibition by SKF differ by more than 2 orders of magnitude for the two current components. Therefore, the GABA concentration dependencies could be described phenomenologically by a Michaelis-Menten equation with apparent $K_m$ values ($K_m^{app}$):

$$v = V_{max} \frac{\frac{[GABA]}{K_m^{app}}}{1 + \frac{[GABA]}{K_m^{app}}}$$

When the dependence of rate of GABA uptake on GABA concentration was determined in the absence and the presence of 25 $\mu$M SKF, the competitive inhibition of GABA uptake became apparent (Fig. 4A). The addition of 25 $\mu$M SKF shifted the $K_m^{app}$ (uptake) from 62 to 138 $\mu$M. Inhibition of GABA uptake by SKF was voltage-independent; GABA uptake experiments under voltage-clamp control at $-20$ and $-60$ mV resulted in the same $IC_{50}$ (uptake) value of 54 $\mu$M SKF (data not shown). Figure 4B shows the dependence of GABA-evoked current on GABA concentration in the absence of SKF and in the presence of 0.5 and 25 $\mu$M SKF. The addition of 0.5 $\mu$M SKF shifted the $K_m^{app}$ (current) from 17 to 41 $\mu$M; the addition of 25 $\mu$M SKF shifted the $K_m^{app}$ (current) further to 152 $\mu$M. $K_m^{app}$ (current) in the absence of SKF does not change in the voltage range from 0 to $-30$ mV; at more negative potentials, $K_m^{app}$ (current) increases to a value of 50 $\mu$M at a potential of $-150$ mV. $K_m^{app}$ (current) in the presence of 25 $\mu$M SKF does not change over the entire voltage range from 0 to $-110$ mV.

In the absence of GABA, voltage jumps applied to mGAT1-expressing oocytes induced voltage-dependent transient currents generated by the binding of extracellular $Na^+$ (Mager et al., 1993; Liu et al., 1998). These mGAT1-mediated transient currents were nearly abolished by only 2 $\mu$M SKF (Fig. 5A). This becomes apparent in the plot of voltage dependence of the charge movement as well (Fig. 5B). Because the transient current is associated with the transition between two discrete states of the mGAT1 ($Na^+$-bound and $Na^+$-unbound state), the voltage-dependence of the charge movement can be described by Fermi equation according to the following:

$$Q_{transient} = \frac{Q_{max} - Q_{min}}{1 + e^{(E - E_{1/2}) z_F F/RT}} + Q_{min}$$

with $Q_{transient}$ representing the charges moved in response to the potential step; $Q_{max}$ and $Q_{min}$ representing the maximal and minimal charge movements, respectively; $E$ is the potential; $E_{1/2}$ is the potential causing half-maximal charge movement; and $z_F$ is the effective valency of the moved charges per transporter. $F/RT$ has its usual thermodynamical meaning. $Q_{max} = N \times e_0 \times z_F$ is a measure for the amount of mGAT1 that can bind $Na^+$ (with $N$ representing the number of transporters and $e_0$ the elementary charge), and $E_{1/2}$ gives a measure for the $Na^+$ affinity (Liu at al., 1998). The data for the

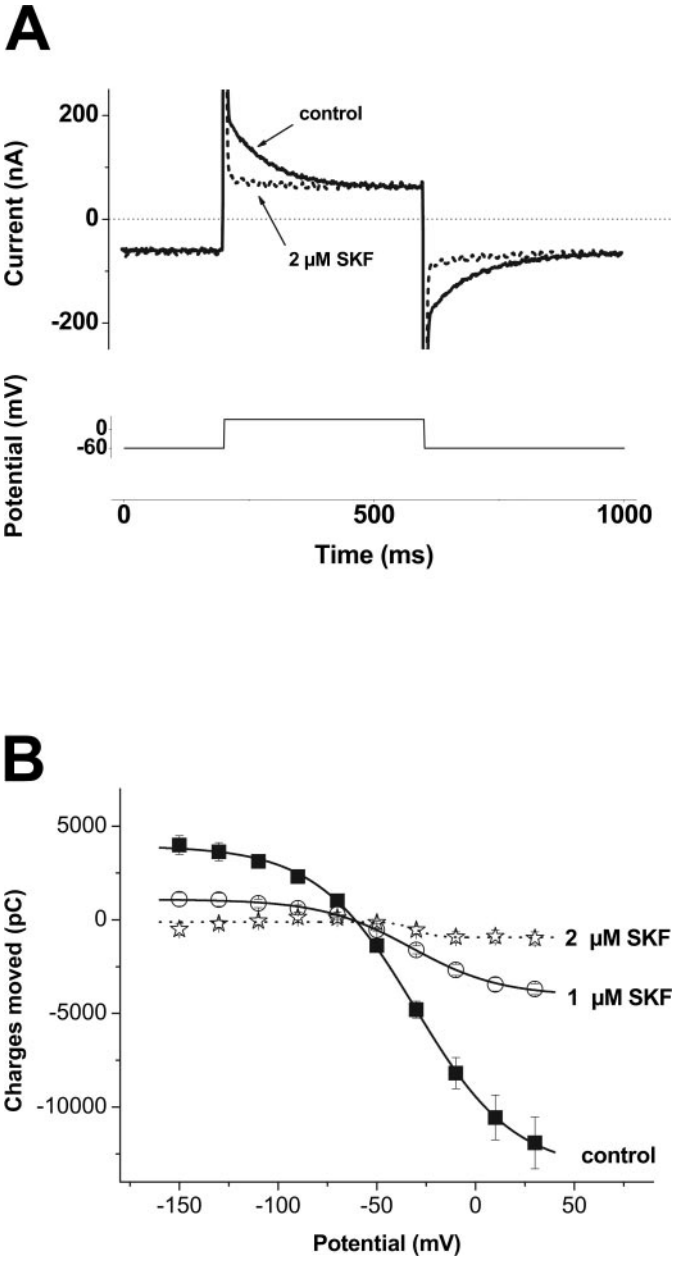


**Fig. 5.** Transient current and charge movements. A, typical current responses of a single mGAT1-expressing oocyte in the absence of GABA to a 400-ms voltage pulse from $-60$ to $+30$ mV. The solid line represents the current in the absence of SKF, the broken line represents the current in the presence of 2 $\mu$M SKF. Because of the scaling, the capacitive peaks of the oocyte are cut. B, ■, moved charges in the absence of SKF, ○, moved charges in the presence of 1 $\mu$M SKF, and ⋆, moved charges in the presence of 2 $\mu$M SKF. Data are averages from four to eight oocytes ± S.E.M. The lines are fits according to Fermi equation (eq. 4). Fit parameters are given in the text.

voltage dependence of the charge movement in the absence of SKF could be fitted with $Q_{max}$ = 17.3 ± 0.4 nA, $z_F$ = 1.00 ± 0.04, and $E_{1/2}$ = −30.5 ± 1.2 mV; the data in the presence of 1 μM SKF could be fitted with $Q_{max}$ = 5.1 ± 0.3 nA, $z_F$ = 0.90 ± 0.12, and $E_{1/2}$ = −32.0 ± 3.2 mV. Given errors are reduced $\chi^2$ errors. A fit of the charge voltage dependence in the presence of 2 μM SKF was not possible because of its very low amplitude.

The uptake of GABA is coupled to the cotransport of $Na^+$ and $Cl^-$; a stoichiometry of 1 GABA:2 $Na^+$:1 $Cl^-$ is usually assumed on the basis of Hill coefficients for the concentration dependencies (Kavanaugh et al., 1992) and on the basis of estimations of rate of uptake for the substrates (Keynan and Kanner, 1988; see *Discussion*). We determined the rates of GABA, $Na^+$, and $Cl^-$ uptake by radioactive tracer measurements on the same batches of oocytes and under identical conditions (Fig. 6). In the absence of SKF, the ratio of GABA to $Na^+$ and $Cl^-$ was 1:4.3:1.3. In the presence of 25 μM SKF, neither GABA nor $Cl^-$ uptake was significantly affected, but $Na^+$ uptake decreased by a factor of 2, resulting in a transport ratio of GABA to $Na^+$ and $Cl^-$ of 1:2.2:1. No GABA-induced $^{86}Rb^+$ uptake could be detected (data not shown). Neither $Na^+$ efflux (in the presence of 10 μM ouabain) nor $Cl^-$ efflux could be observed (data not shown).

## Discussion

In this study, we investigated the current components of the GABA transporter GAT1. By means of two-electrode voltage clamp, radioactive tracer measurements, and pharmacological separation, we could identify two independent current components of the GABA-evoked current.

**The Components of GABA-Evoked Current.** The large difference between the currents calculated from GABA uptake (representing just the transport current) and the measured current (representing the GABA-evoked current) in Fig. 1B clearly indicates that the GABA-evoked current cannot be attributed solely to GABA transport coupled to cotransport of $Na^+$ and $Cl^-$ at a fixed stoichiometry of 1 GABA:2 $Na^+$:1 $Cl^-$. The fact that the GABA-evoked current was 3 to 5 times larger than the calculated transport current (Fig. 1B) can be explained either by an additional current component not linked to the transport or by the existence of a variable transport stoichiometry as described by Cammack et al. (1994), yielding another number of transported ions than assumed in our calculation. Four of our experimental results are consistent with the view that the GABA-evoked current is composed of a component from a fixed 1:2:1 stoichiometry plus an additional current component. The different $K_m$ values for uptake and GABA-evoked current (Table 1) indicate that GABA transport and parts of the GABA-evoked current are uncoupled from each other (Ingram et al., 2002). In addition, GABA uptake and GABA-evoked current are inhibited differently by GABA-analogous inhibitors such as NA and SKF (Figs. 2 and 3), strongly suggesting different underlying processes; the discrepancy of the $IC_{50}$ values of our study from that of others (Borden, 1996) can be explained by the different experimental conditions. The SKF dependence of the GABA-evoked current can only be described by the sum of two independent inhibitory reactions (eq. 2), whereas the SKF dependence of GABA uptake could be perfectly described with a single inhibitory reaction (eq. 1). Finally, the $K_m$ values for GABA uptake and GABA-evoked current in the presence of 25 μM SKF are nearly identical (Table 1), and the current-voltage dependencies of the calculated current and the GABA-evoked current in the presence of 25 μM SKF can be superimposed (Fig. 1B). This shows that the GABA-evoked current in the absence of SKF consists of a transport current and a second current component, which is independent of the transport of GABA (the transmitter-gated current) and which can be blocked by 25 μM SKF. It should be noted that at 400 μM GABA, the rate of uptake is not significantly affected by the presence of 25 μM SKF, but the GABA-evoked current is decreased by a factor of 3.

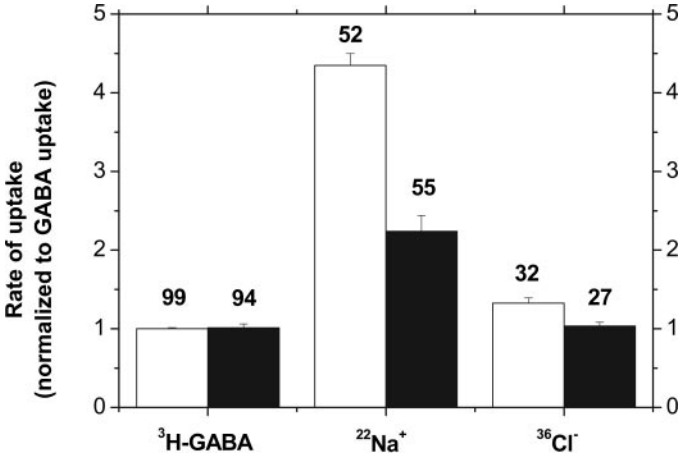


**Fig. 6.** [$^3$H]GABA, $^{22}Na^+$, and $^{36}Cl^-$ uptakes. □, the uptake in presence of 400 μM GABA only. ■, the uptake in the presence of 25 μM SKF and 400 μM GABA. The uptake of each substrate is normalized to the rate of GABA-uptake in the absence of SKF. One unit corresponds to a rate of uptake of 247 ± 3 fmol/s. The numbers above the bars indicate the number of oocytes. Error bars are S.E.M. To eliminate uptake via non-GAT1 pathways, rates of uptake from control oocytes were subtracted from the rates of uptake from mGAT1-expressing oocytes.

The fact that Hilgemann and colleagues (Hilgemann and Lu, 1999; Lu and Hilgemann, 1999a,b) could not find evidence for additional current components may be explained by the excised patch technique they used. The giant patch is lacking all cytoplasmic compounds which possibly regulate the functions of membrane proteins. This, on the other hand, indicates a possible dependence of the transmitter-gated current on cytoplasmic factors.

**Separation of the Components.** SKF and NA inhibit the GABA-evoked current at more than 1 order of magnitude lower concentrations than the rate of uptake (Fig. 3). Because NA has been demonstrated to be transported by the GAT1 (Kanner et al., 1983) and to evoke an $Na^+$-dependent current (data not shown), for further investigations, we concentrated on the effects of SKF. To quantify the effects of SKF on GABA concentration dependencies of uptake and GABA-evoked current (Fig. 4, A and B) we fitted the respective results with eq. 3. The identical $V_{max}$ values, the parallel shift of the curves, and the increase of the $K_m^{app}$ value for the rate of uptake (Fig. 4A, eq. 3) from 62 to 138 μM GABA by the addition of 25 μM SKF supports the competitive inhibition of GABA transport. In addition, the GABA concentration-dependence of the GABA-evoked current is shifted; in this case, we observed a shift of $K_m^{app}$ from 17 to 42 μM upon application of 0.5 μM SKF and to 152 μM upon application of 25 μM SKF (Fig. 4B, eq. 3). It is noted that Fig. 4B superficially resembles the

TABLE 1
Fitted parameters for GABA and SKF dependencies of rate of GABA uptake and GABA-evoked current
The given errors are reduced $\chi^2$ errors derived by least square fittings of averaged values (Origin 7.0).

| | Rate of Uptake | | | Current | | |
|---|---|---|---|---|---|---|
| | *μM* | *Fit* | | *μM* | *Fit* | |
| $K_m$ | 62 ± 7 | Eq. 3 | Fig. 4A | 17 ± 1.8 | Eq. 3 | Fig. 4B |
| $K_{m\ (0.5\ \mu M\ SKF)}$ | | | | 42 ± 3 | Eq. 3 | Fig. 4B |
| $K_{m\ (25\ \mu M\ SKF)}$ | 138 ± 15 | Eq. 3 | Fig. 4A | 152 ± 25 | Eq. 3 | Fig. 4B |
| $IC_{50\ (400\ \mu M\ GABA)}$ | 54 | Estimated | Fig. 2 | 1.5 | Estimated | Fig. 2 |
| $K_I^{transp}$ | 7.6 ± 0.15 | Eq. 1 | Fig. 2 | 8.8 ± 3.7 | Eq. 2 | Fig. 2 |
| $K_I^{trans\text{-}gated}$ | | | | 0.03 ± 0.004 | | |

situation in which SKF, acting like a noncompetitive antagonist on GABA transporters, causes a shift in the agonist (GABA) dose-response curve in the presence of spare GABA transporters. At a low concentration (0.5 μM), SKF would cause a parallel shift, and at high concentration (25 μM), SKF would cause a reduction in the maximum response. However, the presence of spare GABA transporters can be ruled out because, as shown in Fig. 4A, at high concentrations (25 μM), SKF caused only a parallel shift in the GABA uptake rate. Therefore, the best explanation for the SKF effect observed in Fig. 4B is that SKF competitively antagonized a transport current component and noncompetitively antagonized a transmitter-gated current component of the GABA-evoked current. Thus, a combination of 400 μM GABA and 25 μM SKF can be used to separate the transport current from the transmitter-gated current. Further evidence for this conclusion is the fact that in the presence of 25 μM SKF, the apparent $K_m^{app}$ values for rate of uptake and GABA-evoked current are nearly identical; that means the two $K_m$ values in the presence of 25 μM SKF represent the GABA transport process. Also the fact that the calculated current (representing the transport current) and GABA-evoked current in the presence of 25 μM SKF can be superimposed strongly supports this conclusion.

**The SKF Binding.** How can we explain that SKF inhibits the GABA-evoked current with two different $K_I$ values (0.03 and 8.8 μM)? It is most likely that SKF acts competitively on the GABA transport and allosterically on the transmitter-gated current. This idea is particularly supported by the competitive and noncompetitive inhibition pattern in Fig. 4, A and B, but also by the inhibition of the voltage-dependent charge movements (Fig. 5). The voltage dependence of charge movements in the presence of 1 μM SKF shows only reduced amplitude; the other parameters defining the shape of the sigmoidal curve are identical with those in the absence of SKF. This indicates a reduced number of $Na^+$-binding GAT1 in the presence of 1 μM SKF and may be attributed to a potential-independent binding of SKF to an allosteric binding site. Because PMZ is relatively ineffective in blocking the GABA-evoked current and GABA transport, and, on the other hand, NA and SKF sharing the structural moiety block the GABA-evoked current and GABA transport differentially, it is likely that the allosterically acting moiety of SKF is similar to NA (Fig. 3). The observation that 2 μM SKF can abolish the transient current whereas the GABA-evoked current is inhibited by only 50% may be attributed to a competitive inhibition of the GABA transport.

**The Stoichiometry of Transport.** On the basis of uptake measurements of substrates (Keynan and Kanner, 1988) and analysis of the respective Hill coefficients for GABA-evoked currents (Kavanaugh et al., 1992), a transport stoichiometry of 1 GABA:2 $Na^+$:1 $Cl^-$ was suggested. In the presence of 25 μM SKF and 400 μM GABA, the only GAT1-mediated activity is the GABA transport mode, and the current measured under these conditions matches the current calculated from the rate of GABA uptake on the basis of one positive net charge being transported into the cell per GABA molecule taken up (Fig. 1B). Our tracer flux measurements under identical experimental conditions with [$^3$H]GABA, $^{22}Na^+$, and $^{36}Cl^-$ directly demonstrate that for 1 GABA transported into the cell, 2 $Na^+$ and 1 $Cl^-$ are taken up (Fig. 6). Neither $Na^+$ nor $Cl^-$ efflux could be observed.

The tracer uptake measurements (Fig. 6) yielded that 25 μM SKF is not only inefficient to block GABA uptake at 400 μM GABA, but the $Cl^-$ uptake is hardly affected. On the other hand, $Na^+$ uptake is strongly reduced, whereas $^{86}Rb^+$ translocation is not affected, and extracellular $Ca^{2+}$ (J. Fei, personal communication) and changes in pH (Cao et al., 1997; Forlani et al., 2001) do not alter GABA-evoked currents. These observations indicate that the SKF-sensitive transmitter-gated current is carried by $Na^+$ ions. The reduction of $Na^+$ uptake by 25 μM SKF fits well with the reduction of GABA-evoked current by a factor of 3 in potential range of −20 to −40 mV (Fig. 1B). However, because of the imprecise superimposition of the calculated current-voltage curve and the current-voltage curve in the presence of 25 μM SKF between −60 and −80 mV (Fig. 1B), we believe that without further experiments, it is not reasonable to assume an $Na^+$-selective conductance pathway.

## Conclusion

We demonstrated that the GABA-evoked current in *X. laevis* oocytes is composed of two independent components, the transport current that originates from the 1 GABA:2 $Na^+$:1 $Cl^-$ stoichiometry, and the transmitter-gated current that is mediated by an $Na^+$ conductance pathway. SKF is a useful tool to separate these two components because it inhibits them in a different manner and thus offers the possibility to investigate the transmitter-gated current in a physiological environment.

#### Acknowledgments

The assistance by Heike Biehl, Heike Fotis, and Boris Schlaak is gratefully acknowledged. We thank Drs. Chau Wu and Yani Zhu for helpful discussions and critical reading of the manuscript.

#### References

Aragon C and Lopez-Corcuera B (2003) Structure, function and regulation of glycine neurotransporters. *Eur J Pharmacol* **479:**249–262.

Borden LA (1996) GABA transporter heterogeneity: pharmacology and cellular localization. *Neurochem Int* **29:**335–356.
Borden LA, Murali-Dhar TG, Smith KE, Weinshank RL, Branchek TA, and Gluchowski C (1995) Tiagabine, SKF 89976-A, CI-966 and NNC-711 are selective for the cloned GABA transporter GAT-1. *Eur J Pharmacol* **14:**219–224.
Cammack JN, Rakhilin SV, and Schwartz EA (1994) A GABA transporter operates asymmetrically and with variable stoichiometry. *Neuron* **13:**949–960.
Cammack JN and Schwartz EA (1996) Channel behavior in a γ-aminobutyrate transporter. *Proc Natl Acad Sci USA* **93:**723–727.
Cao Y, Mager S, and Lester HA (1997) $H^+$ permeation and pH regulation at a mammalian serotonin transporter. *J Neurosci* **17:**2257–2266.
Eckstein-Ludwig U, Fei J, and Schwarz W (1999) Inhibition of uptake, steady-state currents and transient charge movements generated by the neuronal GABA transporter by various anticonvulsant drugs. *Br J Pharmacol* **128:**92–102.
Forlani G, Bossi E, Ghirardelli R, Giovannardi S, Binda F, Bonadiman L, Ielmini L, and Peres A (2001) Mutation K448E in the external loop 5 of rat GABA transporter rGAT1 induces pH sensitivity and alters substrate interactions. *J Physiol* **15:**479–494.
Galli A, Blakely RD, and Defelice LJ (1996) Norepinephrine transporters have channel modes of conduction. *Proc Natl Acad Sci USA* **93:**8671–8676.
Galli A, Defelice LJ, Duke BJ, Moore KR, and Blakely RD (1995) Sodium-dependent norepinephrine-induced currents in norepinephrine-transporter-transfected HEK-293 cells blocked by cocaine and antidepressants. *J Exp Biol* **198:**2197–2212.
Galli A, Petersen CI, DeBlaquiere M, Blakely RD, and Defelice LJ (1997) *Drosophila* serotonin transporters have voltage-dependent uptake coupled to a serotonin-gated ion channel. *J Neurosci* **17:**3401–3411.
Grossman TR and Nelson N (2002) Differential effect of pH on sodium binding by the various GABA transporters expressed in *Xenopus* oocytes. *FEBS Lett* **527:**125–132.
Hilgemann DW and Lu CC (1999) GAT1 (GABA:$Na^+$:$Cl^-$) cotransport function. Database reconstruction with an alternating access model. *J Gen Physiol* **114:**459–475.
Ingram SL, Prasad BM, and Amara SG (2002) Dopamine transporter-mediated conductances increase excitability of midbrain dopamine neurons. *Nat Neurosci* **5:**971–978.
Kanner BI (1978) Active transport of gamma-aminobutyric acid by membrane vesicles isolated from rat brain. *Biochemistry* **17:**1207–1211.
Kanner BI, Bendahan A, and Radian R (1983) Efflux and exchange of γ-aminobutyric acid and nipecotic acid catalysed by synaptic plasma membrane vesicles isolated from immature rat brain. *Biochim Biophys Acta* **731:**54–62.
Kavanaugh MP, Arriza JL, North RA, and Amara SG (1992) Electrogenic uptake of γ-aminobutyric acid by a cloned transporter expressed in *Xenopus* oocytes. *J Biol Chem* **267:**22007–22009.
Keynan S and Kanner BI (1988) γ-Aminobutyric acid transport in reconstituted preparations from rat brain: Coupled sodium and chloride fluxes. *Biochemistry* **27:**12–17.
Lafaire AV and Schwarz W (1986) Voltage dependence of the rheogenic $Na^+/K^+$ ATPase in the membrane of oocytes of *Xenopus laevis*. *J Membrane Biol* **91:**43–51.
Liu Y, Eckstein-Ludwig U, Fei J, and Schwarz W (1998) Effect of mutation of glycosylation sites on the $Na^+$ dependence of steady-state and transient currents generated by the neuronal GABA transporter. *Biochim Biophys Acta* **1415:**246–254.
Loo DDF, Eskandari S, Boorer KJ, Sarkar HK, and Wright EM (2000) Role of $Cl^-$ in electrogenic $Na^+$-coupled cotransporters GAT1 and SGLT1. *J Biol Chem* **275:**37414–37422.
Lu CC and Hilgemann DW (1999a) GAT1 (GABA:$Na^+$:$Cl^-$) cotransport function. Steady state studies in giant *Xenopus* oocyte membrane patches. *J Gen Physiol* **114:**429–444.
Lu CC and Hilgemann DW (1999b) GAT1 (GABA:$Na^+$:$Cl^-$) cotransport function. Kinetic studies in giant *Xenopus* oocyte membrane patches. *J Gen Physiol* **114:**445–457.
Mager S, Min C, Henry DJ, Chavkin C, Hoffman BJ, Davidson N, and Lester HA (1994) Conducting states of a mammalian serotonin transporter. *Neuron* **12:**845–859.
Mager S, Naeve J, Quick M, Labarca C, Davidson N, and Lester HA (1993) Steady-states, charge movements and rates for a cloned GABA transporter expressed in *Xenopus* oocytes. *Neuron* **10:**177–188.
Masson J, Sagné C, Hamon M, and El Mestikawy S (1999) Neurotransmitter transporters in the central nervous system. *Pharmacol Rev* **51:**439–464.
Nelson N (1998) The family of $Na^+/Cl^-$ Neurotransmitter transporters. *J Neurochem* **71:**1785–1803.
Risso S, Defelice LJ, and Blakely RD (1996) Sodium-dependent GABA-induced currents in GAT1-transfected HeLa cells. *J Physiol* **490:**691–702.
Sonders MS and Amara SG (1996) Channels in transporters. *Curr Opin Neurobiol* **6:**294–302.
Sonders MS, Zhu SJ, Zahniser NR, Kavanaugh MP, and Amara SG (1997) Multiple ionic conductances of the human dopamine transporter: The actions of dopamine and psychostimulants. *J Neurosci* **17:**960–974.
Supplisson S and Roux MJ (2002) Why glycine transporters have different stoichiometries. *FEBS Lett* **529:**93–101.

**Address correspondence to:** Dr. Stephan Krause, University of Oulu, Department of Physical Sciences, Division of Biophysics, Linnanmaa, 90014 Oulun Yliopisto, Finland. E-mail: stephan.krause@oulu.fi